Defining the Retinoid Binding Site in the Rod Cyclic Nucleotide-gated Channel

Diana M. Horrigan,[1] Michelle L. Tetreault,[1] Natia Tsomaia,[1] Chrysoula Vasileiou,[2] Babak Borhan,[2] Dale F. Mierke,[1] Rosalie K. Crouch,[3] and Anita L. Zimmerman[1]

[1]Department of Molecular Pharmacology, Physiology, and Biotechnology, Brown Medical School, Providence, RI 02912
[2]Department of Chemistry, Michigan State University, East Lansing, MI 48824
[3]Department of Ophthalmology, Medical University of South Carolina, Charleston, SC 29425

Rod vision is initiated when 11-cis-retinal, bound within rhodopsin, absorbs a photon and isomerizes to all-trans-retinal (ATR). This triggers an enzyme cascade that lowers cGMP, thereby closing cyclic nucleotide-gated (CNG) channels. ATR then dissociates from rhodopsin, with bright light releasing millimolar levels of ATR. We have recently shown that ATR is a potent closed-state inhibitor of the rod CNG channel, and that it requires access to the cytosolic face of the channel (McCabe, S.L., D.M. Pelosi, M. Tetreault, A. Miri, W. Nguitragool, P. Kovithvathanaphong, R. Mahajan, and A.L. Zimmerman. 2004. *J. Gen. Physiol.* 123:521–531). However, the details of the interaction between the channel and ATR have not been resolved. Here, we explore the nature of this interaction by taking advantage of specific retinoids and retinoid analogues, namely, β-ionone, all-trans-C15 aldehyde, all-trans-C17 aldehyde, all-trans-C22 aldehyde, all-trans-retinol, all-trans-retinoic acid, and all-trans-retinylidene-*n*-butylamine. These retinoids differ in polyene chain length, chemical functionality, and charge. Results obtained from patch clamp and NMR studies have allowed us to better define the characteristics of the site of retinoid–channel interaction. We propose that the cytoplasmic face of the channel contains a retinoid binding site. This binding site likely contains a hydrophobic region that allows the ionone ring and polyene tail to sit in an optimal position to promote interaction of the terminal functional group with residues ~15 Å away from the ionone ring. Based on our functional data with retinoids possessing either a positive or a negative charge, we speculate that these amino acid residues may be polar and/or aromatic.

The Journal of General Physiology

INTRODUCTION

Cyclic nucleotide-gated (CNG) channels mediate the light response in retinal rods and cones. Rod CNG channels are thought to be tetramers consisting of one β (CNGB1) and three α (CNGA1) subunits (Weitz et al., 2002; Zheng et al., 2002; Zhong et al., 2003), each with a cyclic nucleotide binding domain on its cytoplasmic COOH terminus. Gating of these channels is modulated by several factors including phosphorylation enzymes (Gordon et al., 1992; Molokanova et al., 1997), calcium binding proteins (Matulef and Zagotta, 2003; Trudeau and Zagotta, 2003), and by retinoids, specifically all-trans-retinal (ATR) (Dean et al., 2002; McCabe et al., 2004).

ATR is a member of the retinoid family, a class of compounds that includes vitamin A and its derivatives (Nau and Blaner, 1999). These compounds are known to regulate such physiological processes as gene transcription and immune responses, and play a major role in visual transduction. During visual transduction in rods, the chromophore 11-cis-retinal photoisomerizes to ATR and is then released from its binding pocket in opsin. A bright light is thought to cause the release of millimolar levels of ATR (Saari, 1999). Although much of the ATR is likely buffered by membranes and proteins within the outer segment, some is expected to be accessible to the CNG channels located in the nearby plasma membrane.

We have shown that ATR can inhibit cloned rod CNG channels (Dean et al., 2002; McCabe et al., 2004). This inhibition is potent, especially at low, near physiological levels of cGMP, in which case it inhibits in the nanomolar range. ATR is a closed-state inhibitor that prefers unliganded channels and has profound effects on the channel's cGMP sensitivity. Previous work also suggests that ATR requires access to the intracellular surface of the channel (McCabe et al., 2004), which implies that inhibition by ATR is not the result of a nonspecific bilayer effect. However, it is still unclear whether the inhibition involves nonspecific hydrophobic interactions between ATR and the channel, or whether the channel contains a specific retinoid binding site. In this study we have used retinoid analogues to explore this question

Correspondence to Anita L. Zimmerman: Anita_Zimmerman@brown.edu

The online version of this article contains supplemental material.

Abbreviations used in this paper: ATR, all-trans-retinal; ATR-NBu, all-trans-retinylidene-*n*-butylamine; ATRol, all-trans-retinol; CNG, cyclic nucleotide-gated; DPC, dodecylphosphocholine; NMR, nuclear magnetic resonance.

in more detail. We used retinoid analogues of differing polyene chain lengths, namely, β-ionone, and all-trans-C15, all-trans-C17, and all-trans-C22 aldehydes (see Fig. 1), which have been used by others to explore the mechanism of opsin activation (Jin et al., 1993; Buczylko et al., 1996; Kefalov et al., 1999; Crouch et al., 2002). We also have used all-trans-retinoic acid and all-trans-retinylidene-*n*-butylamine to investigate the role of charge in the inhibition. Our results suggest that the inhibitory effect of retinoids is not merely the result of nonspecific hydrophobic interactions with the channel. Instead, there is likely a binding site with specific length and charge requirements necessary for retinoids to inhibit the rod CNG channel.

MATERIALS AND METHODS

Expression of Channels in *Xenopus* Oocytes

The CNG channel clone for the bovine rod α subunit (CNGA1; GenBank/EMBL/DDBJ accession no. NM-174278) was provided by W.N. Zagotta (University of Washington, Seattle, WA) (in the pGEMHE plasmid). The pGEMHE plasmid contains the untranslated sequence of the *Xenopus* β-globin gene to promote high protein expression in oocytes (Liman et al., 1992). Channel cRNA was made by in vitro transcription using Ambion's mMessage mMachine™ kit. Partial ovariectomies were performed on anesthetized *Xenopus laevis* frogs, and individual oocytes were isolated by treatment with ~1 mg/ml collagenase type 1A (Sigma-Aldrich) in a low-calcium solution (82.5 mM NaCl, 2.5 mM KCl, 5 mM HEPES, 1 mM $MgCl_2$ at pH 7.6) for ~1 h. Channel cRNA was injected into oocytes using a Drummond "NANOJECT" injector. Typically, ~50 nl of 1 μg/μl CNGA1 cRNA was injected into each egg. Injected oocytes were incubated at 16°C for 3–12 d before patch clamp experiments. Oocytes were stored in a solution containing: 96 mM NaCl, 2 mM KCl, 1.8 mM $CaCl_2$, 5 mM HEPES, 1 mM $MgCl_2$, 2.5 mM pyruvic acid, 100 U/ml penicillin, and 100 μg/ml streptomycin, at pH 7.6. The vitelline membrane was removed by mechanical dissection after treatment with a hypertonic solution containing 100 mM *N*-methyl-D-glucamine, 2 mM KCl, 10 mM EGTA, 10 mM HEPES, and 1 mM $MgCl_2$, at pH 7.4.

Electrophysiological Solutions and their Application

All-trans-retinal, all-trans-retinol, all-trans-retinoic acid, and β-ionone were purchased from Sigma-Aldrich. All-trans-C15, all-trans-C17, and all-trans-C22 aldehydes were produced in Dr. Crouch's lab. The synthesis of these retinoids has been described previously (Buczylko et al., 1996). All-trans-retinylidene-*n*-butylamine was produced in Dr. Borhan's lab following the methods of Govardhan and Oprian (Govardhan and Oprian, 1994). See Fig. 1 for the molecular structure of each compound. The cell chamber for patch clamp experiments was a glass Petri dish. Water soluble solutions were applied using a 36-solution patch perfusion system, RSC-100 rapid solution changer (Molecular Kinetics). Both sides of the patches were bathed in a low-divalent sodium solution consisting of 130 mM NaCl, 500 μM EDTA, and 2 mM HEPES, at pH 7.2. The solution bathing the intracellular surface of the patch contained 2 mM cGMP (Sigma-Aldrich) dissolved in the low-divalent solution. Niflumic acid (500 μM; Sigma-Aldrich) was added to the extracellular solution to block Ca^{2+}-activated Cl^- channels endogenous to *Xenopus* oocytes. For retinoids stored in benzene, nitrogen gas was used to evaporate the benzene before preparation of a retinoid stock in ethanol. All retinoid stocks were made in 100% ethanol and kept in amber glass vials covered in aluminum foil and stored at −80°C or −20°C until use. The purity and stability of the stocks were checked by measuring absorption spectra (200–800 nm) with a Beckman DU640 spectrophotometer. Retinoids were applied to the intracellular surface of patches by removing ~50% of the bath volume, vigorously mixing the retinoid stock into this solution using a glass Pasteur pipette in a glass beaker, and then pouring this solution back into the remaining bath and mixing again. We found that the greatest concentration of ethanol applied to any patch had no effect on cGMP-activated current or on the seal resistance. Petri dishes and agar bridges were replaced after each experiment. ATR degradation was checked spectroscopically under both dim and bright room light conditions. Under dim room light no degradation was seen; however, degradation was apparent in brighter room light. Thus, for all retinoid experiments, dim room light was used.

Electrophysiological Recordings and Analysis

Standard patch clamp methods were used to record currents from excised, inside-out patches. Pipette openings were typically 0.5–5 μm in diameter with resistances of 1.0–15 MΩ after fire polishing. All recordings were obtained at room temperature. Currents were recorded in response to 200-ms voltage pulses ranging from −100 to +100 mV in 50-mV steps from a holding potential of 0 mV; or, where indicated, 1.5-s pulses to +100, +50, −50, or −100 mV from a holding potential of 0 mV. Leak currents were measured in the low divalent solution without cGMP and were subtracted from each record. All currents were measured in the steady state after completion of voltage-dependent gating (Karpen et al., 1988) and before significant ion depletion (Zimmerman et al., 1988).

Retinoids were added to patches only after allowing for completion of the spontaneous increases in apparent cGMP affinity of the rod channel due to dephosphorylation by endogenous patch-associated phosphatases (Gordon et al., 1992; Molokanova et al., 1997). This increase in apparent cGMP affinity took tens of minutes and was monitored by sampling the current periodically at a cGMP concentration (typically 10 μM) that was below the $K_{1/2}$, while incubating the patch the rest of the time in saturating cGMP (2 mM) to accelerate the process (Molokanova et al., 1999).

For retinoid dose–response relations, the bath (i.e., intracellular surface of the patch) contained a saturating concentration of cGMP (2 mM). The current was monitored for ~1 h after each addition of retinoid to ensure that steady state had been reached (see Fig. S1 for representative time course plots of several retinoids used in this study, available at http://www.jgp.org/cgi/content/full/jgp.200509387/DC1). Typically one or two retinoid concentrations were tested per patch. For most patches, the leak was rechecked at the end of the experiment by applying the low divalent solution to the patch through a glass capillary tube anchored in the bath and attached to a syringe.

Patch currents were recorded using an Axopatch 1B or 200 patch clamp amplifier (Axon Instruments, Inc.) with analogue-to-digital converters connected to a Macintosh Quadra or G4 computer running Pulse software (Instrutech). The data were low-pass filtered at 2 kHz and sampled at 10 kHz. Data analysis was performed using the IgorPro software package (WaveMetrics). All data points used in the dose–response relations were measured at +100 mV in saturating (2 mM) cGMP at the indicated retinoid concentration. All points shown are averages of several patches. Smooth curves are fits with the Hill equation: $IN/IN_{max} = [Ret]^n/(IC_{50}{}^n + [Ret]^n)$, where IN = percent inhibition, IN_{max} = maximal percent inhibition, IC_{50} = concentration of retinoid required for half maximal inhibition, Ret = retinoid or retinoid analogue, and n is the Hill coefficient.

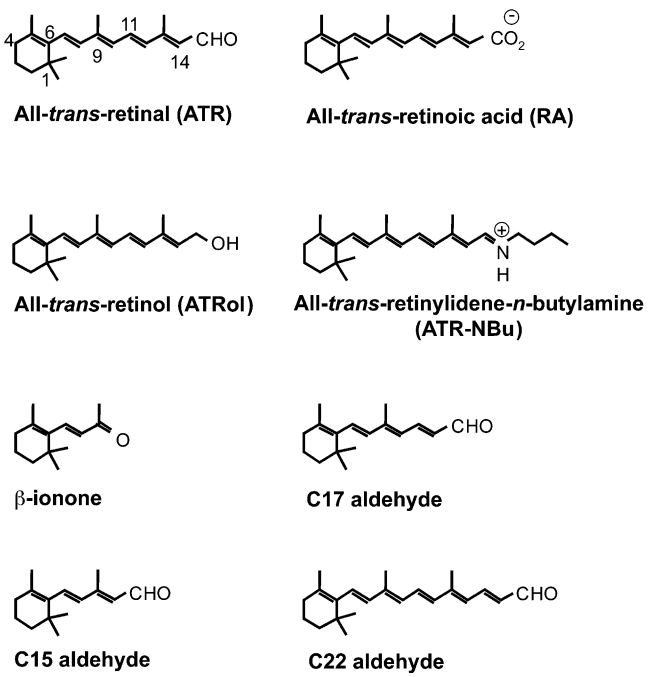

Figure 1. Structures of retinoids and retinoid analogues. All-trans-retinal (ATR), all-trans-retinol (ATRol), β-ionone, all-trans-C15 aldehyde, all-trans-retinoic acid (RA), all-trans-retinylidene-*n*-butylamine (ATR-NBu), all-trans-C17 aldehyde, and all-trans-C22 aldehyde. (All-trans-C15, C17, and C22 aldehydes are named based on the total number of carbons, including methyl groups, as per Buczylko et al., 1996. Though depicted as charged, the actual charge states of RA and ATR-NBu within the retinoid binding site are not known.)

Nuclear Magnetic Resonance

Retinoids were examined by NMR in aqueous solution. Initially, the powdered form of the retinoid was dissolved in DMSO to make a concentrated stock. Separately, 180 mM DPC solution (dodecylphosphocholine-*d38*) was prepared in 20 mM phosphate buffer at pH 7.0. The retinoid stock was added to 600 μl buffer containing micelles to obtain a final retinoid concentration of 2 mM.

All NMR experiments were collected at 298 K on a 600 MHz Bruker Avance spectrometer. The reported chemical shift values for ^{1}H were expressed in ppm and referenced to the ^{1}H resonance from TSP at 0.0 ppm. Two-dimensional total correlation spectroscopy (TOCSY) was performed with a mixing time of 35 ms. The spin lock field was 10 kHz. The water signal was suppressed using a WATERGATE sequence. For radical-induced relaxation, the 16-doxylstearic acid was solubilized in methanol-d_4 to a final concentration of 60 mM. 5 μl of this solution was added to the retinoid/DPC solution. TOCSY experiments were recorded under identical conditions before and after the addition of the doxylstearic acid. Intensities of the peaks were measured before and after addition of the doxylstearic acid (van de Ven et al., 1993; Pellegrini et al., 1998).

Online Supplemental Material

Fig. S1 (available at http://www.jgp.org/cgi/content/full/jgp.200509387/DC1) shows representative time course plots for ATR, all-trans-retinol (ATRol), and C22 aldehyde applied to inside-out patches in the presence of saturating (2 mM) cGMP. In each case, the inhibition reached steady state over the course of ~1 h.

RESULTS

We have previously shown that ATR can inhibit the rod CNG channel (Dean et al., 2002; McCabe et al., 2004). Here, we examine the structural features of ATR responsible for the inhibition with the long-range aim of determining the site of interaction of ATR with the channel. ATR is composed of an ionone ring and a hydrophobic nine-carbon long chain with conjugated double bonds ending in an aldehyde group (see Fig. 1). Several retinoids and retinoid analogues were employed in this study; their structures are shown in Fig. 1.

The first structural feature examined was the polyene chain length. β-ionone, the compound with the shortest polyene chain, was unable to inhibit the rod CNG channel at concentrations as high as 10 μM in saturating (2 mM) cGMP (Fig. 2 A). This concentration of β-ionone far exceeds the IC_{50} (220 nM) for inhibition of the channel by ATR (McCabe et al., 2004). What about compounds with polyene chain lengths between those of β-ionone and ATR? As seen in Fig. 1, C15 and C17 aldehydes are four and two carbons shorter than ATR, respectively. As illustrated in Fig. 2 (B and C), C15 and C17 aldehydes gave little, if any, inhibition of the channel, even at concentrations (1 μM) much larger than the IC_{50} for ATR. Since the critical micellar concentration of ATRol is reported to be 2 μM (Noy, 1999), higher concentrations of C15 and C17 aldehyde were not applied to patches due to the potential formation of micelles in solution.

We next tested C22 aldehyde, a retinoid with a polyene chain that is two carbons longer than ATR. Fig. 3 A shows a representative patch where 400 nM C22 aldehyde produced 46% inhibition in the presence of saturating (2 mM) cGMP. Fig. 3 B shows a dose–response relation for this inhibition. Although the IC_{50} for C22 aldehyde (415 nM) is almost twice that of the IC_{50} for ATR, C22 aldehyde can still be considered a potent inhibitor. The Hill coefficient for C22 aldehyde ($n = 2.5$) predicts a steeper curve than that predicted for ATR ($n = 1.4$; McCabe et al., 2004); however, it is not clear whether this difference is meaningful, since it may reflect limitations in our ability to accurately measure this parameter for such slow, lipophilic inhibitors.

These results imply that there is a critical chain length necessary for inhibition of the channel. There are two possible reasons why polyene chain length might be important in inhibition, the first of which seems more likely: (1) the channel may have a specific retinoid binding site that dictates a preferred distance between the ionone ring and the terminal functional group; (2) partitioning of retinoids into hydrophobic regions of the channel may be the determining factor in their inhibitory ability. In the latter case, shorter retinoids (β-ionone, C15, and C17 aldehyde) would inhibit the channel less efficiently than longer retinoids

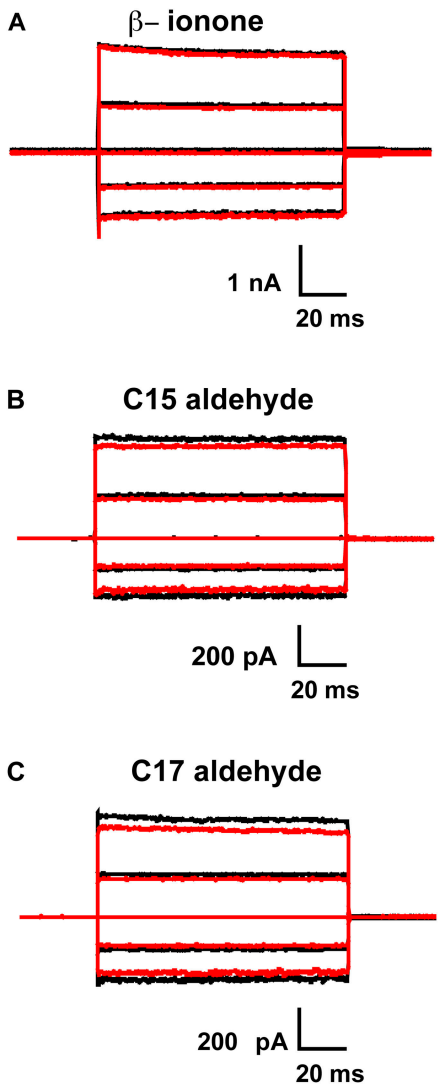

Figure 2. β-Ionone, and C15 and C17 aldehydes do not significantly inhibit the homomeric rod CNG channel in the presence of saturating cGMP. Currents were measured from multichannel, inside-out patches of homomeric (CNGA1) rod channels at saturating (2 mM) cGMP. The raw traces represent families of cGMP-activated currents in response to voltage steps ranging from −100 to +100 mV in 50-mV increments from a holding potential of 0 mV. Currents measured in the absence of cGMP were subtracted from all traces. Black traces represent currents before the addition of the indicated retinoid; red traces represent currents after 1 h (steady state) in the indicated retinoid. Similar results for β-ionone, C15, and C17 aldehyde were obtained with 9, 3, and 15 patches, respectively. (A) There was no change in current with 10 μM β-ionone. (B) Currents were reduced by 8% in 1 μM C15 aldehyde. (C) Currents were reduced by 11.5% in 1 μM C17 aldehyde.

(ATR and C22 aldehyde), since they would not be expected to partition as effectively. This hypothesis would also predict that C22 would be a better inhibitor than ATR, since its polyene chain is longer by two carbons. The finding that C22 is a less effective inhibitor than ATR suggests that hydrophobic partitioning of retinoids is not the main determinant of inhibitor potency.

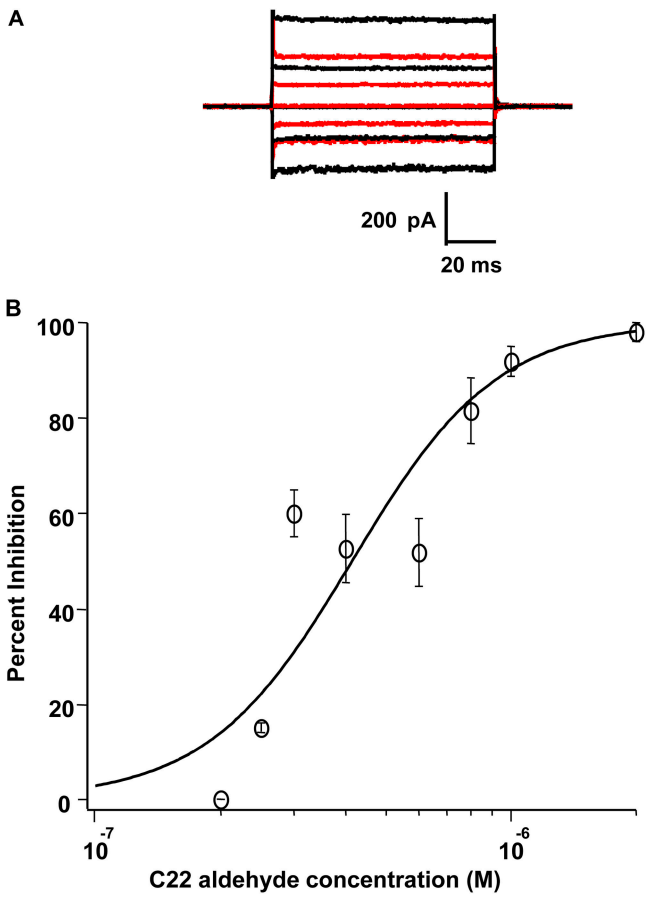

Figure 3. C22 aldehyde is a potent inhibitor of the homomeric rod CNG channel. (A) The raw traces represent families of cGMP-activated currents in response to voltage steps ranging from −100 to +100 mV in 50-mV increments from a holding potential of 0 mV. Currents measured in the absence of cGMP were subtracted from all traces. Black traces represent currents in saturating cGMP before the addition of C22 aldehyde; red traces represent currents after 1 h (steady state) in 400 nM C22 aldehyde (46% inhibition). (B) The dose–response relation for C22 aldehyde inhibition of the rod CNG channel. All points were measured at +100 mV after 1 h (steady state) in the indicated concentration of C22 aldehyde and saturating (2 mM) cGMP. Data were normalized to maximal current in 2 mM cGMP in the absence of C22 aldehyde, with leak current in the absence of cGMP subtracted from each trace. Each point is an average from two to three patches, and the smooth curve is a fit with the Hill equation, where the IC_{50} = 415 nM, and n = 2.5.

Additional evidence that ATR likely inhibits via a specific binding site within the channel comes from studies using nuclear magnetic resonance (NMR). The relative partitioning of ATR and C17 aldehyde was measured in dodecylphosphocholine (DPC) micelles, using nitroxide radical–induced relaxation of the ^{1}H NMR signals of the retinoids following standard procedures (Pellegrini et al., 1998). Both ATR and C17 aldehyde were found to readily incorporate into the DPC micelle, based on the increase in NMR line width. Upon addition of 16-doxylstearic acid to the solution, which

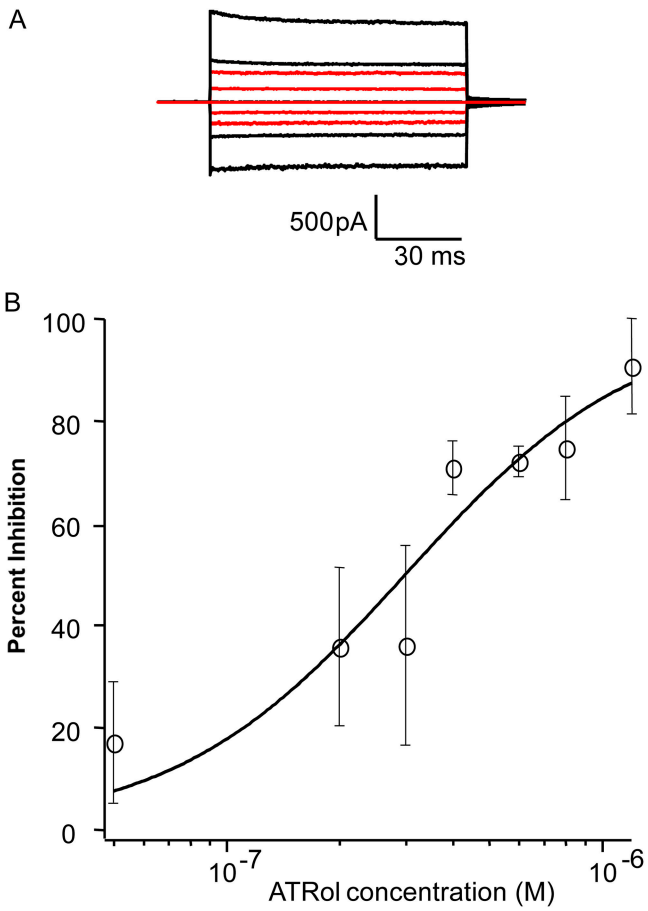

Figure 4. ATRol is a potent inhibitor of the homomeric rod CNG channel. (A) The raw traces represent families of cGMP-activated currents in response to voltage steps ranging from −100 to +100 mV in 50-mV increments from a holding potential of 0 mV. Currents measured in the absence of cGMP were subtracted from all traces. Black traces represent currents in saturating cGMP (2 mM) before the addition of ATRol; red traces represent currents after 1 h (steady state) in 400 nM ATRol (63% inhibition). (B) The dose–response relation for ATRol inhibition of the rod CNG channel. All points were measured at +100 mV after 1 h (steady state) in the indicated concentration of ATRol and saturating (2 mM) cGMP. Data were normalized to maximal current in 2 mM cGMP in the absence of ATRol, with leak current in the absence of cGMP subtracted from each. Each point is an average from two to four patches, and the smooth curve is a fit with the Hill equation, where the IC_{50} = 300 nM, and n = 1.4.

places the nitroxide radical approximately in the core of the micelle (van de Ven et al., 1993), the NMR signals for both ATR and C17 aldehyde are diminished, indicating close proximity to the electron radical. The ^{1}H signals for the ATR are reduced by ∼56% on average upon the addition of the 16-doxylstearic acid; the radical-induced relaxation for C17 aldehyde is similar or even greater for some protons. These results indicate that although C17 aldehyde is shorter, its partitioning into the zwitterionic micelles of DPC is similar to that of ATR. Therefore, the ability of ATR to inhibit the channel potently, while C17 aldehyde demonstrates no inhibition, is likely due to a specific channel–retinoid interaction and is not solely determined by hydrophobic partitioning.

Considering our results with C22 aldehyde and the NMR data, it seems likely that retinoids interact with the channel via a specific binding site. To test whether the terminal functional group affects this interaction, we first compared inhibition by ATRol with that by ATR (see Fig. 1 for structures). Fig. 4 A shows a representative family of traces in response to 400 nM ATRol, and Fig. 4 B shows the dose–response relation for ATRol inhibition. Based on the IC_{50} values of ATR and ATRol (220 and 300 nM respectively), it seems that ATR may be only slightly more potent than ATRol.

We next examined retinoid analogues with terminal functional groups that may carry a negative (all-trans-retinoic acid [RA]) or a positive (all-trans-retinylidene-*n*-butylamine [ATR-NBu]) charge (see DISCUSSION). Fig. 5 A shows that 400 nM RA did not inhibit the channel. If the site contains aromatic and/or polar residues, then ATR-NBu should be a very effective inhibitor. Fig. 5 B (top) shows a representative family of traces in which 80 nM ATR-NBu conferred 60% inhibition in the presence of saturating (2 mM) cGMP. ATR-NBu was a much more potent inhibitor than any other retinoid tested (see Table I). These results suggest that the retinoid binding site prefers a positively charged over a negatively charged functional group. It is possible that ATR-NBu is acting as a slow voltage-dependent blocker like dequalinium (Rosenbaum et al., 2003, 2004), at a site distinct from the retinoid binding site. However, this does not seem to be the case. Fig. 5 B (bottom) shows a representative set of traces from the same patch as that shown in the top panel, in which each voltage pulse was applied for 1.5 s in the presence of 80 nM ATR-NBu and 2 mM cGMP after steady state was reached. There is no slow increase in current at negative voltages, or decrease in current at positive voltages characteristic of voltage-dependent blockers like dequalinium (Rosenbaum et al., 2004). Thus, ATR-NBu does not appear to be a slow voltage-dependent blocker, but instead most likely inhibits via the same mechanism as the other retinoids tested.

DISCUSSION

We have shown that a hydrophobic polyene chain length of at least nine carbons is essential for retinoid inhibition of the rod CNG channel. Retinoids with shorter chains, specifically β-ionone, and C15 and C17 aldehydes, are not able to significantly inhibit the channel. In contrast, ATR, C22 aldehyde, and ATRol, all with longer polyene chains, are potent inhibitors. We have provided two lines of evidence suggesting that hy-

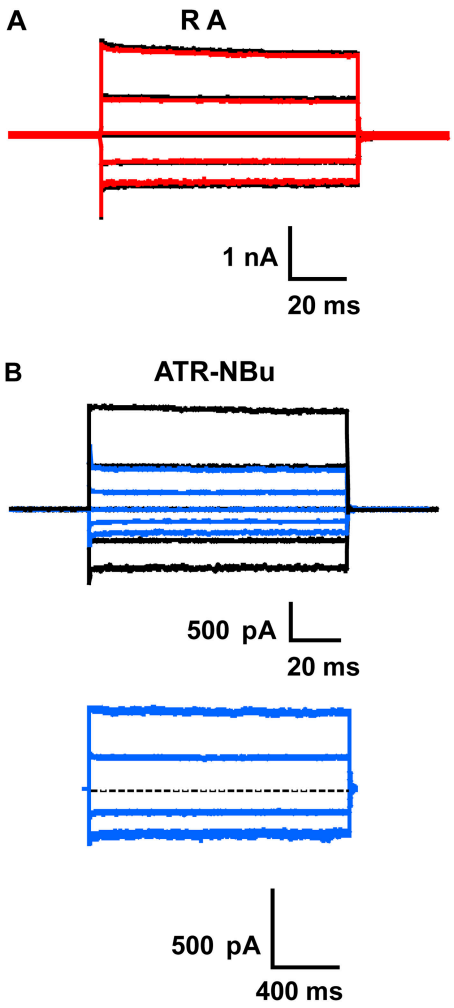

Figure 5. RA does not inhibit the homomeric rod CNG channel; ATR-NBu does inhibit, but not in a voltage-dependent way. Currents were measured from multichannel, inside-out patches of homomeric (CNGA1) rod channels at saturating (2 mM) cGMP. The raw traces in A and B (top) represent families of cGMP-activated currents in response to voltage steps ranging from −100 to +100 mV in 50-mV increments from a holding potential of 0 mV. Currents measured in the absence of cGMP were subtracted from all traces. The traces in B (bottom) represent cGMP-activated currents in response to longer (1.5 s) voltage pulses to +100, +50, −50, or −100 mV from 0 mV after inhibition in 80 nM ATR-NBu reached steady state. The dashed line represents the baseline (i.e., zero current). The holding potential was 0 mV during the application of ATR-NBu. Black traces represent currents in saturating cGMP prior to the addition of RA or ATR-NBu; red or blue traces represent currents after 1 h in RA or ATR-NBu, respectively. (A) 400 nM RA gave no inhibition (red); similar results were seen in two other patches. (B, top) 80 nM ATR-NBu conferred 60% inhibition (blue); (bottom) 1.5-s voltage pulses on the same patch as in the top panel after 1 h in 80 nM ATR-NBu do not show any voltage dependence of ATR-NBu inhibition.

drophobic partitioning alone is not the active mechanism for retinoid inhibition of the rod CNG channel. First, C22 aldehyde is a slightly less potent inhibitor than ATR (see Table I); and second, NMR studies indicate that ATR and C17 aldehyde partition similarly into DPC micelles. These results suggest a specific interaction between the retinoid and the channel, likely via a retinoid binding site. Although we cannot rule out the possibility that retinoids inhibit by binding to an intermediary protein, this possibility seems unlikely since we have measured quantitatively similar retinoid inhibition of CNG channels in patches pulled from rod outer segments (unpublished data).

TABLE I

Chain Length and Inhibitory Potency of Retinoid Analogues

Retinoid	Distance from carbon 4 to carbon 15 (Å)	Inhibitory potency
β-ionone	7.55	No inhibition
C15 aldehyde	10.06	No inhibition
C17 aldehyde	12.58	No inhibition
C22 aldehyde	17.5	IC_{50} = 415 nM
ATR[a]	15	IC_{50} = 220 nM
ATRol	15	IC_{50} = 300 nM
RA (−)	15	No inhibition
ATR-NBu (+)[b]	15	IC_{50} = ∼80 nM

[a]IC_{50} from McCabe et al. (2004).
[b]Distance from C4 to C15 is 15 Å, but butylamine chain extends past the functional group (Fig. 1).

The analogues examined here allow for some definition of the putative retinoid binding site. The length of the polyene chain, measured from carbon 4 (located at the side of the ionone ring farthest from the aldehyde group) to the oxygen bound to carbon 15 (see Fig. 1), provides valuable insight into the requirements for channel inhibition. Table I presents an estimate of this length for each analogue. The retinoids with lengths that are <15 Å (β-ionone, and C15 and C17 aldehydes) do not inhibit, whereas C22 aldehyde (17.5 Å distance) does inhibit, but not as well as ATR, ATRol, or ATR-NBu (each with a 15-Å distance). This suggests that the binding site prefers retinoids with a terminal functional group ∼15 Å removed from carbon 4.

Taken together, these data suggest that the channel has a retinoid binding site that likely contains two regions that are a preferred distance (15 Å) apart. One region constrains the ionone ring while holding the hydrophobic tail in an optimal position for interaction of the terminal functional group with residues located at the second region 15 Å away. As the distance between the ionone ring and the terminal functional group increases or decreases (i.e., if the hydrocarbon tail is shortened or lengthened), this interaction is diminished and the inhibition reduced or ablated. However, we do not yet know whether the ionone ring structure per se is required for inhibition, since a series of retinoids lacking the ionone ring have not yet been tested.

We have also shown that the identity of the functional group located at the end of the polyene chain is very im-

portant in the inhibition, and therefore can speculate about the nature of the residues within the channel that may be involved in the inhibition. Since ATRol is approximately as potent an inhibitor as ATR, it seems unlikely that formation of a Schiff base within the binding site is the active mechanism for inhibition. Our results with RA and ATR-NBu provide evidence that the binding site likely contains polar and/or aromatic amino acid residues. However, further experiments are required to test this hypothesis, since the charge states of ATR-NBu and RA within the binding site are not known. Finally, our results with ATR-NBu suggest that the binding site is not sterically limited immediately after the second interaction site; the structure of ATR-NBu extends several carbons beyond the 15-Å point (at which its functional group is located), and yet it is a potent inhibitor.

Since we have previously shown that ATR requires access to the intracellular side of the channel in order to confer inhibition (McCabe et al., 2004), it seems plausible that the retinoid binding site is located on the intracellular side of the channel, such as in the cytosolic NH_2 or COOH terminus. Alternatively, the site could lie between neighboring subunits, or in other regions that are associated with the membrane surface and are accessible only from the intracellular side. Since ATR-NBu, and previously ATR (McCabe et al., 2004), showed no voltage dependence, it is unlikely that the retinoid binding site lies within the membrane electric field. The identity of the amino acids within this retinoid interaction site and their exact location within the channel structure remain to be determined. However, it seems reasonable to propose that the retinoid binding site is hydrophobic and has two key regions of interaction: the first of which constrains the ionone ring and hydrocarbon tail, while the second site is 15 Å removed from this site and interacts with the terminal functional group via polar and/or aromatic residues. This interaction with the terminal functional group is essential for inhibition.

We thank Dr. Sarah L. McCabe for participating in a few of the early experiments, Dr. Gabe Travis for helpful discussions, and Mandy Barragan and Jin Huang for technical assistance.

This work was supported by the National Institutes of Health grants EY07774 (A.L. Zimmerman), GM067311 (B. Borhan), GM54082 (D.F. Mierke), EY12231 (R.K. Crouch) and EY04939 (R.K. Crouch), and an unrestricted grant to Medical University of South Carolina from Research to Prevent Blindness (RPB), Inc., (R.K. Crouch); R.K. Crouch is an RPB Senior Scientific Investigator.

Olaf S. Andersen served as editor.

Submitted: 16 August 2005
Accepted: 16 September 2005

REFERENCES

Buczylko, J., J. Saari, R. Crouch, and K. Palczewski. 1996. Mechanisms of opsin activation. *J. Biol. Chem.* 271:20621–20630.

Crouch, R.K., V. Kefalov, W. Gartner, and M.C. Cornwall. 2002. Use of retinal analogues for the study of visual pigment function. *Methods Enzymol.* 343:29–48.

Dean, D.M., W. Nguitragool, A. Miri, S.L. McCabe, and A.L. Zimmerman. 2002. All-trans-retinal shuts down rod cyclic nucleotide-gated ion channels: a novel role for photoreceptor retinoids in the response to bright light? *Proc. Natl. Acad. Sci. USA.* 99:8372–8377.

Gordon, S.E., D.L. Brautigan, and A.L. Zimmerman. 1992. Protein phosphatases modulate the apparent agonist affinity of the light-regulated ion channel in retinal rods. *Neuron.* 9:739–748.

Govardhan, C.P., and D. Oprian. 1994. Active site-directed inactivation of constitutively active mutants of rhodopsin. *J. Biol. Chem.* 269:6524–6527.

Jin, J., R. Crouch, D.W. Corson, B.M. Katz, E.F. MacNichol, and M.C. Cornwall. 1993. Noncovalent occupancy of the retinal-binding pocket of opsin diminishes bleaching adaptation of retinal cones. *Neuron.* 11:513–522.

Karpen, J.W., A.L. Zimmerman, L. Stryer, and D.A. Baylor. 1988. Gating kinetics of the cyclic GMP-activated channel of retinal rods: flash photolysis and voltage-jump studies. *Proc. Natl. Acad. Sci. USA.* 85:1287–1291.

Kefalov, V., M. Cornwall, and R. Crouch. 1999. Occupancy of the chromophore binding site of opsin activates visual transduction in rod photoreceptors. *J. Gen. Physiol.* 113:491–503.

Liman, E.R., J. Tytgat, and P. Hess. 1992. Subunit stoichiometry of a mammalian K^+ channel determined by construction of multimeric cDNAs. *Neuron.* 9:861–871.

Matulef, K., and W.N. Zagotta. 2003. Cyclic nucleotide-gated ion channels. *Annu. Rev. Cell Dev. Biol.* 19:23–44.

McCabe, S.L., D.M. Pelosi, M. Tetreault, A. Miri, W. Nguitragool, P. Kovithvathanaphong, R. Mahajan, and A.L. Zimmerman. 2004. All-trans-retinal is a closed-state inhibitor of rod cyclic nucleotide-gated ion channels. *J. Gen. Physiol.* 123:521–531.

Molokanova, E., F. Maddox, C.W. Luetje, and R.H. Kramer. 1999. Activity-dependent modulation of rod photoreceptor cyclic nucleotide-gated channels mediated by phosphorylation of a specific tyrosine residue. *J. Neurosci.* 19:4786–4795.

Molokanova, E., B. Trivedi, A. Savchenko, and R.H. Kramer. 1997. Modulation of rod photoreceptor cyclic nucleotide-gated channels by tyrosine phosphorylation. *J. Neurosci.* 17:9068–9076.

Nau, H., and W.S. Blaner. 1999. Retinoids: The Biochemical and Molecular Basis of Vitamin A and Retinoid Action. Vol. 139. Springer-Verlag, New York. 619 pp.

Noy, N. 1999. Physical-chemical properties and action of retinoids. *In* Retinoids: The Biochemical and Molecular Basis of Vitamin A and Retinoid Action. Vol. 139. H. Nau and W.S. Blaner, editors. Springer-Verlag, New York. 3–29.

Pellegrini, M., A. Bissello, M. Rosenblatt, M. Chorey, and D. Mierke. 1998. Binding domain of human parathyroid hormone receptor: from conformation to function. *Biochemistry.* 37:12737–12743.

Rosenbaum, T., A. Gordon-Shaag, L.D. Islas, J. Cooper, M. Munari, and S.E. Gordon. 2004. State-dependent block of CNG channels by dequalinium. *J. Gen. Physiol.* 123:295–304.

Rosenbaum, T., L.D. Islas, A.E. Carlson, and S.E. Gordon. 2003. Dequalinium: a novel, high-affinity blocker of CNGA1 channels. *J. Gen. Physiol.* 121:37–47.

Saari, J.C. 1999. Retinoids in mammalian vision. *In* Retinoids: The Biochemical and Molecular Basis of Vitamin A and Retinoid Action. Vol. 139. H. Nau and W.S. Blaner, editors. Springer-Verlag, New York. 563–588.

Trudeau, M.C., and W.N. Zagotta. 2003. Calcium/calmodulin modulation of olfactory and rod cyclic nucleotide-gated ion channels. *J. Biol. Chem.* 278:18705–18708.

van de Ven, F., J. van Os, J. Aelen, S. Wymenga, M. Remerowski, R.

Konings, and C. Hilgers. 1993. Assignment of H1, 15N, and backbone 13C resonances in detergent-solubilized M13 coat protein via multinuclear multidimensional NMR: a model for the coat protein monomer. *Biochemistry.* 32:8322–8328.

Weitz, D., N. Ficek, E. Kremmer, P.J. Bauer, and U.B. Kaupp. 2002. Subunit stoichiometry of the CNG channel of rod photoreceptors. *Neuron.* 36:881–889.

Zheng, J., M. Trudeau, and W.N. Zagotta. 2002. Rod cyclic nucleotide-gated channels have a stoichiometry of three CNGA1 subunits and one CNGB1 subunit. *Neuron.* 36:891–896.

Zhong, H., J. Lai, and K.-W. Yau. 2003. Selective heteromeric assembly of cyclic nucleotide-gated channels. *Proc. Natl. Acad. Sci. USA.* 100:5509–5513.

Zimmerman, A.L., J.W. Karpen, and D.A. Baylor. 1988. Hindered diffusion in excised patches from retinal rod outer segments. *Biophys. J.* 54:351–355.